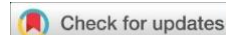


RESEARCH PAPER

OPEN ACCESS



## Exploration of digital filters on cardiac monitor devices equipped with non-invasive blood pressure (NIBP)

Priyambada C. Nugraha<sup>1</sup>, Sumber<sup>1</sup>, Zuva Muzachim<sup>1</sup>, Rifqi Rabani<sup>1</sup>, and Elmira Rofida Alhaq<sup>1,2</sup>, Triwiyanto Triwiyanto<sup>1</sup>, and Vugar Abdullayev<sup>3</sup>

<sup>1</sup> Department of Medical Electronics Technology, Poltekkes Kemenkes Surabaya, Surabaya, Indonesia

<sup>2</sup> Biomedical Engineering Master Degree, Departement of Physics, Faculty of Science and Technology, Surabaya, Indonesia

<sup>3</sup> Department of Computer Engineering, Azerbaijan State Oil and Industry University, Baku, Azerbaijan

### ABSTRACT

Heart disease is a leading cause of global mortality, making accurate monitoring essential for early detection and prevention of complications. Although heart monitoring technology has advanced, there are still limitations in precisely detecting early symptoms. This study aims to develop a Cardiac Monitor device capable of monitoring patients with heart conditions through three main parameters: electrocardiogram (ECG), phonocardiogram (PCG), and non-invasive blood pressure measurement (NIBP). The system designed in this research integrates digital filters, namely Butterworth (order 2, 4, 8) and Kalman, to enhance the quality of ECG and PCG signals. Additionally, the oscillometric method in non-invasive blood pressure measurement (NIBP) is used as a comparison for blood pressure estimation by analyzing the correlation between the R peak on the ECG signal, pulse transit time (PTT), and the first and second heart sounds (S1, S2) on the PCG signal. Blood pressure estimation is performed using algorithmic calculations to determine the accuracy of the design module in measuring systolic and diastolic pressure. The results indicate that the 8th-order Butterworth filter is more effective in reducing noise in ECG and PCG signals compared to the Kalman filter. The study also finds a significant correlation between the R peak on the ECG and the first heart sound on the PCG. The design module's blood pressure measurement errors compared to algorithmic estimates are  $4.54 \pm 4.94$  mmHg for systolic pressure and  $6.57 \pm 3.83$  mmHg for diastolic pressure, which are close to the AAMI standard of  $5 \pm 8$  mmHg. These findings highlight the great potential of the developed Cardiac Monitor device in improving early diagnosis accuracy and heart disease management.

### PAPER HISTORY

Received July 15, 2024

Revised Sept. 23, 2024

Accepted Nov. 24, 2024

### KEYWORDS

Cardiac monitor;  
Heart disease;  
NIBP;  
ECG;  
PCG;

### CONTACT:

<sup>1</sup>elmirarofida.a@gmail.com

## 1. INTRODUCTION

Cardiac monitor is the monitoring of cardiac activity to determine the patient's condition[1][2][3]. The importance of this cardiac monitor is to monitor the work of the heart with various parameters, namely ECG, PCG, and paramedic to know the initial condition of a person's heart condition[4]. This paramedic is blood pressure. Blood pressure is one of the important vital signs[5][6][7]. Electrocardiography (ECG) is a device that records bioelectrical signals caused by electrical activity in the heart. ECG signals have a specific shape that can be

used to determine the health of a person's heart[8][9][10][11]. The electrical and mechanical activity of the heart also involves the process of blood pressure in flowing blood through the heart valves to the chambers of the heart and lungs[4]. According to Bashar et al, the use of PCG in heart disease provides excellent prediction. However, several studies [12][13][14] aimed at developing the technology have found limitations in recognizing symptoms and detecting abnormalities. Phonocardiograph is a technique for recording human heart sounds [15]. Heart sounds are created from blood flowing through the heart chambers as the cardiac valves

**Corresponding author:** Elmira Rofida Alhaq, [elmirarofida.a@gmail.com](mailto:elmirarofida.a@gmail.com), Department of Medical Electronics Technology, Poltekkes Kemenkes Surabaya, Jl. Pucang Jajar Timur No. 10, 60282, Surabaya, Indonesia and Biomedical Engineering Master Degree, Departement of Physics, Faculty of Science and Technology, Surabaya, Indonesia.

**Copyright** © 2024 by the authors. Published by Jurusan Teknik Elektromedik, Politeknik Kesehatan Kemenkes Surabaya Indonesia. This work is an open-access article and licensed under a Creative Commons Attribution-ShareAlike 4.0 International License ([CC BY-SA 4.0](https://creativecommons.org/licenses/by-sa/4.0/)).

open and close during the cardiac cycle. Vibrations of these structures from the blood flow create audible sounds the more turbulent the blood flow, the more vibrations that get created [16]. This heart sound also involves the process of blood pressure [17]. Blood pressure can analyze the difference between normal and abnormal heart conditions. Research shows that classification models that combine ECG and PCG signals achieve higher accuracy than models that rely on either signal individually, especially when combined with NIBP measurements [18]. This can be done by simultaneously displaying heartbeat signals, heart sounds, and blood pressure measurements where blood pressure measurements are taken automatically. The three parameters are interrelated [19], this correlation is very helpful in monitoring the heart condition simultaneously. In monitoring the heart condition simultaneously so as to provide more complete information about the patient's health condition and assist the doctor in determining the appropriate treatment. In this study, digital filters are given to electrocardiograph signals and phonocardiograph signals to produce better signals as a development of previous research [4][12][13][14][20]. A Butterworth digital filter is a type of finite impulse response (FIR) or infinite impulse response (IIR) filter that is designed to provide a maximally flat frequency response in the passband. Recent research highlights the use of Butterworth filters in digital signal processing to remove noise and extract important components. Applied to channel equalization, noise reduction, audio processing, and filtering of biomedical signals such as ECG, EEG, and EMG[21]. In addition, the Kalman filter is an algorithm that estimates the state of a dynamic system from noisy measurements, resulting in more accurate estimates. Several studies have found that employing the Kalman filter notably decreases measurement noise, which enhances the accuracy of parameter indications [22][23].

This research was conducted by referring to reference journals to support research needs. from several existing reference journals, there are several developments in research on Cardiac Monitor and non-invasive blood pressure In 2008 Agnia Nerlika, designed a Personal Computer-based Electrocardiography (ECG) device, this device only displays one parameter, namely the heartbeat signal (ECG). In 2011 Dian Hera, designed a Personal Computer-based Phonocardiography (PCG) device, this device only displays heart sound signals (PCG). In 2018 Monica Simjanoska, conducted research with the title Non-Invasive Blood Pressure Estimation From ECG Using Machine Learning Techniques, with the author's suggestion that further research is needed. In the next year, in 2019 Risa Alvionita, made a device with the title

Design of Cardiac Monitor for Multi Parameters, this research has a relatively large size and does not explain blood pressure even though it is equipped with several body temperature and pulse parameters. In 2020 Tai Le et al, conducted research with the title Continuous Non-Invasive Blood Pressure Monitoring: A Methodological Review on Measurement Techniques. Where blood pressure measurements are taken along with ECG and PCG data collection. In 2021 Amalia & Nashucha, made a Cardiac Monitor device using a Piezoelectric Sensor Through Carotid Pulse without using a digital filter.

Based on the results and identification of the problems above, the purpose of this study is to develop a cardiac parameter monitoring device for ECG, PCG, and NIBP by displaying signals accurately simultaneously. In addition, this study also observes the relationship between ECG, PCG, and NIBP, where variations in NIBP are significantly correlated with changes in ECG and PCG signals. This study aims to develop a cardiac monitor device capable of simultaneously measuring three main parameters: electrocardiogram (ECG), phonocardiogram (PCG), and non-invasive blood pressure (NIBP), using digital filters (Butterworth and Kalman) to improve signal quality. The goal is to produce a practical and efficient device for real-time cardiac condition monitoring. This research is expected to result in a device that provides a significant contribution to the practice of cardiac condition monitoring in healthcare settings.

## 2. MATERIALS AND METHOD

### A. Dataset

This study, data were collected from 10 respondents aged between 18 and 24 years. The resulting dataset includes three main types of physiological data: heart rate, heart sound, and non-invasive blood pressure. Heart rate was measured using the AD8232 sensor, which detects the electrical activity of the heart through electrodes attached to the respondent's body. A comparative study revealed a high positive correlation ( $r=0.9$ ,  $p < 0.001$ ) between ECG readings from the AD8232 and standard clinical ECG monitors. This indicates that the AD8232 is capable of accurately capturing fundamental cardiac signals, making it appropriate for basic monitoring tasks [24]. Heart sound was measured using the GYMAX9814 sensor, which captures the acoustic vibrations generated by heart activity. The MAX9814 exhibits a total harmonic distortion of approximately 0.04%, which suggests it generates a clean output signal with minimal distortion, thereby improving accuracy in high-fidelity audio applications [25]. Non-invasive blood pressure was measured using the MPX5050GP sensor, which operates in conjunction with a cuff attached to the respondent's arm. The data

collected from these sensors form the core of the dataset used for further analysis. Before data collection, the research devices were calibrated using a vital signs monitor to ensure that all sensors functioned according to the established medical standards. The MS400 simulator provides precision ECG calibration with amplitudes of 0.5-2.0 mV and heart rates up to 350 BPM. This simulator serves as an effective tool for learning ECG interpretation and monitoring techniques without risk to live patients [26]. NIBP calibration with integrated Rigel UNI-SIM pump can be set from 0 mmHg to 350 mmHg, allowing blood pressure simulation and leak testing to evaluate monitor performance [27]. Phantom manikins are used for phonocardiogram (PCG) calibration by mimicking the structure and acoustics of the human heart, allowing testing of the device under controlled conditions. This process involves recording sounds from the manikin, analyzing the data to ensure accuracy, and adjusting the device if necessary. A properly calibrated device minimizes the likelihood of measurement errors, leading to more accurate data and enabling more precise diagnoses and clinical decisions. A properly calibrated device minimizes the likelihood of measurement errors, leading to more accurate data and enabling more precise diagnoses and clinical decisions.

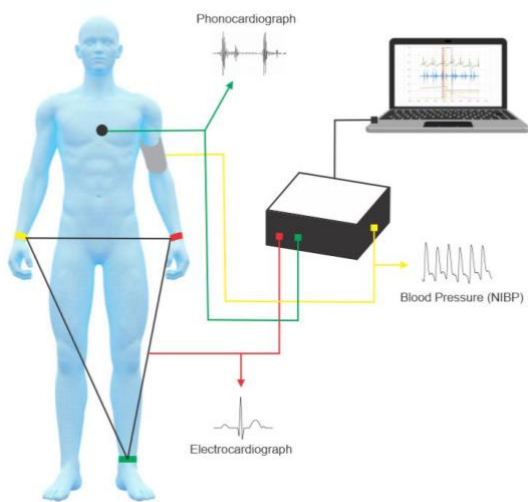


Fig. 1. The implementation of exploration of digital filters on cardiac monitor devices equipped noninvasive blood pressure (NIBP)

## B. Data Collection

Data collection in this study was carried out meticulously to ensure the accuracy and consistency of measurements. The data collection process began with the calibration of the devices using a standardized vital signs monitor. This calibration was essential to align the

sensor measurements with applicable medical standards. After calibration, data were collected from respondents using three main sensors for cardiac condition measurements. ECG, PCG, and blood pressure signals were recorded for 10 seconds until systolic and diastolic blood pressure were determined, with each parameter being measured 5 times and a 20-second rest period between measurements. The recording of ECG and PCG signals consisted of three types of signals: the original signal before filtering, the signal after being filtered using a Butterworth filter and Kalman filter with three different orders, specifically for Butterworth (order 2, order 4, order 8) and Kalman (R:10; Q:1, R:1; Q:1, R:1; Q:0.1). In detail, the total number of cardiac monitor data for one subject is 65 data points.

## C. Data Processing

After data collection is completed, the next step is data processing using the Arduino Uno microcontroller. This microcontroller receives analog signals from the AD8232, GYMAX9814, and MPX5050GP sensors, which are then converted into digital signals for further processing. In this process, the ECG and PCG signals are digitally filtered to reduce noise and enhance signal quality.

The Butterworth filter is used to eliminate unwanted high-frequency components from the signal. This filter has a very smooth frequency response within its passband, and the following equation can express the transfer function of the Butterworth filter:

$$|H(\omega)|^2 = \frac{1}{1 + \left(\frac{\omega}{\omega_p}\right)^{2N}} \quad (1)$$

where  $\omega$  is the angular frequency of the desired signal.  $\Omega_c$  is the cutoff frequency of the filter.  $n$  is the order of the filter. Additionally, the Kalman filter is applied to refine the estimation of the original signal by optimally combining predictions and actual measurements. The Kalman filter operates with two basic equations: prediction and update. The prediction equations are:

$$x_{k-1} = f(x_k, u_k, w_k) \quad (2)$$

where  $x_{k-1}$  is the predicted state at time step  $k - 1$ .  $f(x_k, u_k, w_k)$  is a nonlinear function that describes how the current state  $x_k$ , control input  $u_k$ , and process noise  $w_k$  combine to predict the previous state  $x_{k-1}$ . This equation represents a nonlinear prediction model where the future state is derived from the current state, control input, and noise. It reflects the fact that nonlinear dynamics govern many real-world systems.

**Corresponding author:** Elmira Rofida Alhaq, [elmirarofida.a@gmail.com](mailto:elmirarofida.a@gmail.com), Department of Medical Electronics Technology, Poltekkes Kemenkes Surabaya, Jl. Pucang Jajar Timur No. 10, 60282, Surabaya, Indonesia and Biomedical Engineering Master Degree, Departement of Physics, Faculty of Science and Technology, Surabaya, Indonesia.

**Copyright** © 2024 by the authors. Published by Jurusan Teknik Elektromedik, Politeknik Kesehatan Kemenkes Surabaya Indonesia. This work is an open-access article and licensed under a Creative Commons Attribution-ShareAlike 4.0 International License ([CC BY-SA 4.0](https://creativecommons.org/licenses/by-sa/4.0/)).

$$x_{k-1} = A_k x_k + B_k u_k, w_k \quad (3)$$

where  $x_{k-1}$  is the predicted state at time step  $k - 1$ .  $A_k$  is the state transition matrix, which applies to the current state.  $B_k$  is the control input matrix, which applies to the control input  $u_k$ .  $w_k$  is the process noise at time  $k$ . This equation is the linearized version of the state prediction equation, where the system dynamics are represented by a linear relationship. It is often used when the system can be approximated as linear around a certain operating point.

### 3. RESULTS

#### A. Electrocardiograph (ECG)

The results obtained will show the effect of giving 2 digital filters, namely the Kalman filter and Butterworth filter to the electrocardiogram signal. which will then be analyzed to determine the relationship between the electrocardiograph signal and the phonocardiograph using the best electrocardiograph signal obtained.

Figure 3 shows the frequency response curves of the ECG signal processed using Butterworth bandpass filters with orders 2, 4, and 8, compared to the original unfiltered signal. The study showed that the 8th-order Butterworth filter is very effective at reducing noise, especially in high-frequency ranges above 60Hz, which are typically prone to interference. However, although this higher-order filter (order 8) excels at removing high-frequency components, it also poses the risk of losing important signal details.

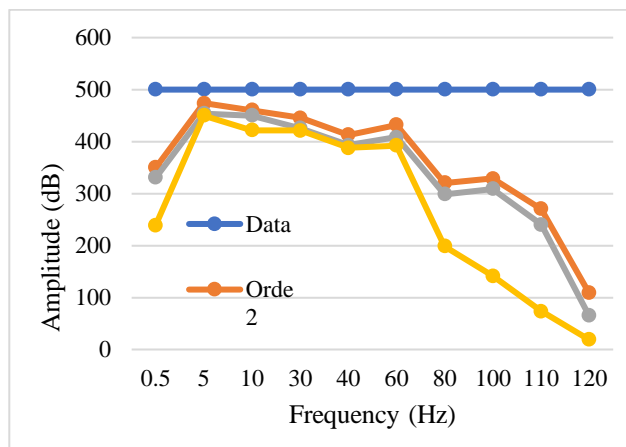


Fig. 3. Butterworth Bandpass Filter Measurement Curve in Research Exploration of Digital Filter on Cardiac Monitor Equipped with Non-Invasive Blood Pressure (ECG)

On the other hand, a lower-order filter (order 2) leads to a more gradual reduction in amplitude, highlighting the need to carefully balance noise reduction with preserving the signal's integrity when selecting the filter order.

Table 1. Butterworth Bandpass Filter Measurement Table in Research Exploration of Digital Filter on Cardiac Monitor Equipped with Non-Invasive Blood Pressure (ECG)

Hz	Data	Orde 2	Orde 4	Orde 8
0,5	500	350,06	330,9	238,8
5	500	474	453,72	449,87
10	500	460,56	449,98	421,6
30	500	445,89	425,65	412
40	500	412,56	393,87	387,69
60	500	432,24	408,6	392,15
80	500	320,49	298,65	198,82
100	500	328,87	308,76	141,54
110	500	270,65	240,46	73,81
120	500	108,65	64,98	18,89

Table 1 shows the measurement results of the Butterworth Bandpass filter with frequency points ranging from 0.5-120 Hz and with an amplitude at each frequency of 5 Volts. Measurements using the Arduino serial monitor with a 9600 baud rate, the measurement results of the frequency points were passed to the Butterworth Bandpass Filter with different order values, namely, Butterworth Bandpass Filter with order 2, Butterworth Bandpass Filter with order 4, and Butterworth Bandpass Filter with order 8. The measurement results of the frequency points after going through the Butterworth Bandpass Filter can be seen in Figure 3.

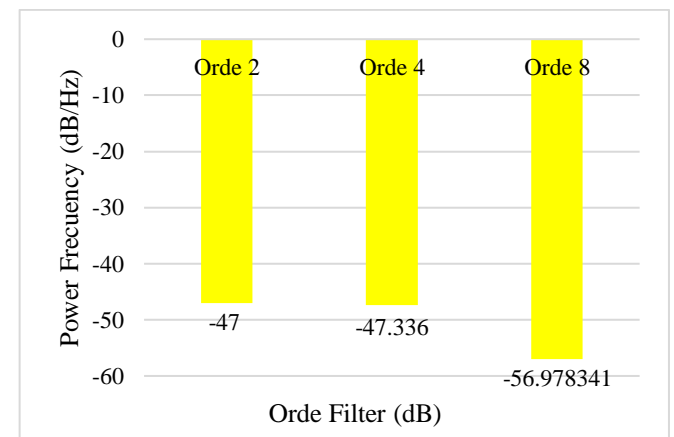


Fig. 4. PSD Result of Butterworth Filter on ECG Signal in Research Exploration of Digital Filter on Cardiac Monitor Equipped with NonInvasive Blood Pressure (ECG)

Figure 4 shows a Power Spectral Density (PSD) graph of the Butterworth Bandpass filter with three different orders: 2, 4, and 8. Each bar in the graph represents the power per frequency (in dB/Hz) produced by the filter for each respective order. The filter with order 2 yields a PSD value of around -47 dB, order 4 around -47.336 dB, and order 8 around -56.978 dB. This graph illustrates that the higher

the order of the filter, the greater the reduction in power of the signal after passing through the filter.

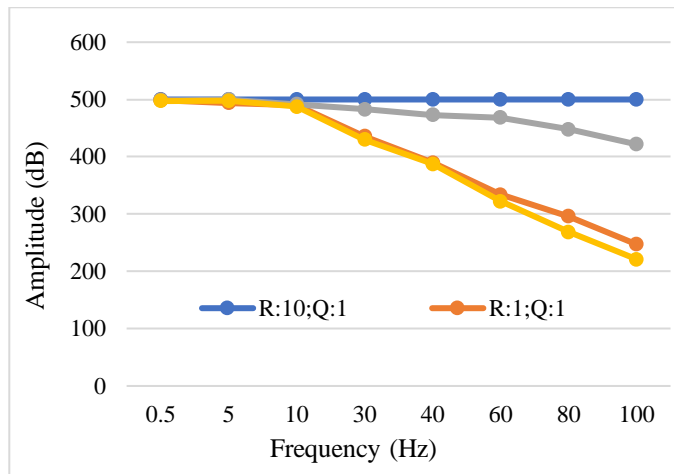


Fig. 5. Kalman Filter Measurement Curve in Research Exploration of Digital Filter on Cardiac Monitor Equipped with Non-Invasive Blood Pressure (ECG)

Figure 5 shows measurement curves using the Kalman Filter on ECG signals from a cardiac monitor equipped with a non-invasive blood pressure device. The Kalman filter with the R:1; Q:0.1 configuration is most effective in reducing noise at mid to high frequencies, with a PSD of -31.73 dB, because it relies more on measurements to aggressively reduce noise. However, at low frequencies, the filter does not change much of the original signal such as the QRS and T waves, which are already strong with little noise, only a small amount of noise reduction occurs. There are four curves showing different configurations of R (process noise variance) and Q (measurement noise variance) values: R:10; Q:1, R:1; Q:1, R:1; Q:0.1, as well as the original unfiltered data. The original data appears stable, while the Kalman Filter results show a decrease in the measured values as the frequency increases, with variations depending on the combination of R and Q used. This illustrates how the Kalman Filter affects signal processing in the context of cardiac monitoring.

Table 2. Kalman Filter Measurement Table in Research Exploration of Digital Filter on Cardiac Monitor Equipped with Non-Invasive Blood Pressure (ECG)

Hz	Data	R:10;Q:1	R:1;Q:1	R:1;Q:0,1
0,5	500	498,76	498,8	497,54
5	500	494	499,7	497,87
10	500	490,64	491,87	487,6
30	500	435,91	482,65	430
40	500	389,75	473,11	387,69
60	500	334,12	468,6	322,15
80	500	296,29	447,95	268,76
100	500	247,2	421,76	221,24

Table 2 shows the results of Kalman filter measurements with frequency points ranging from 0.5-120 Hz and with an amplitude at each frequency of 5 Volts. Measurement using Arduino serial monitor with 9600 baud rate. The measurement results of the frequency points were passed to the Kalman Filter with different coefficient values, namely, Kalman Filter with coefficient R:10 and Q:1, Kalman Filter with coefficient R:1 and Q:1, and Kalman Filter with coefficient R:1 and Q:0.1. The measurement results of the frequency points after going through the Kalman filter can be seen in Figure 5.

Figure 6 shows the Power Spectral Density (PSD) graph of the signal processed with a Kalman filter using three different configurations: R:1;Q:1, R:10;Q:1, and R:1;Q:0.1. Each configuration yields different PSD values, with R:1;Q:1 around -26.266 dB, R:10;Q:1 around -28.402 dB, and R:1;Q:0.1 around -31.736 dB. Lower PSD values indicate greater noise reduction, suggesting that the configuration with R:1;Q:0.1 is the most effective at suppressing noise in the signal. This graph illustrates how variations in the R and Q parameters in the Kalman filter affect the quality of the processed signal.

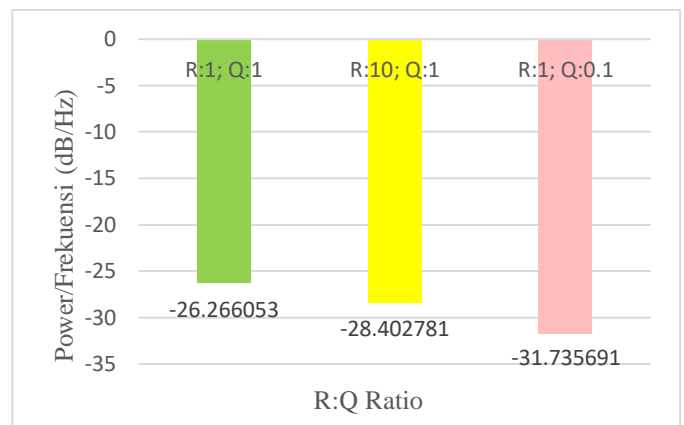


Fig. 6. PSD Result of Kalman Filter on ECG Signal in Research Exploration of Digital Filter on Cardiac Monitor Equipped with Non-Invasive Blood Pressure (ECG)

## B. Phonocardiograph (PCG)

The obtained results will reveal the impact of applying two digital filters, namely the Kalman filter and the Butterworth filter, on the phonocardiogram signal. Further analysis will be conducted to investigate the relationship between the phonocardiogram signal and the electrocardiogram. Figure 7 shows the results of the human heart sound signal before filtering and after filtering. In a study focusing on phonocardiogram (PCG) signal processing for cardiac monitors equipped with non-invasive blood pressure measurement, two types of digital filters, namely Kalman and Butterworth, were used to analyze the difference in effectiveness in clarifying the signal. The PCG signal

measurement results were processed through three stages: raw PCG signal, signal after processing using the Kalman filter, and signal processed using the Butterworth filter.

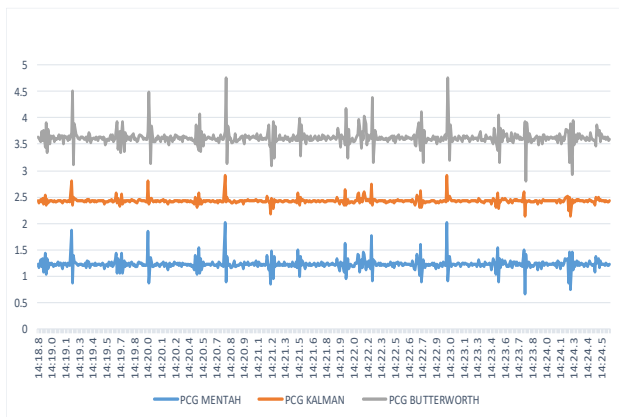


Fig. 7. Original PCG signal (blue), with Kalman Filter (orange), with Butterworth (grey)

The data showed that the amplitude of the raw PCG signal, which had not undergone any processing, had an average amplitude of about 1.22698. This reflects the original signal with unfiltered noise. After applying the Kalman filter, the average amplitude increased to 2.4265, indicating an improvement in signal quality with reduced noise and smoother amplitude fluctuations. However, the Butterworth filter, with an order of 8, resulted in a further increase in amplitude with an average of 3.62454. This filter showed the ability to process the signal more effectively, increasing the amplitude more clearly than the Kalman filter. These results suggest that the Butterworth filter tends to be more aggressive in reducing noise or perhaps accentuating certain signal components, resulting in a clearer PCG signal. This facilitates further analysis of the relationship between cardiac signals and blood pressure, which may be useful for improving accuracy in non-invasive cardiac monitoring systems.

Table 3 presents the measurement results of the phonocardiogram (PCG) signal processed using two types of digital filters, namely the Kalman filter and the Butterworth filter, within the context of research focusing on a cardiac monitor equipped with non-invasive blood pressure measurement. The table includes three main columns: Raw PCG, which shows the amplitude values of the unfiltered signal; Kalman PCG, which shows the values after the signal has been processed with the Kalman filter; and Butterworth PCG, which shows the values after processing with the Butterworth filter.

Table 3. Butterworth and Kalman Filter Measurement Table in Research Exploration of Digital Filter on Cardiac Monitor Equipped with Non-Invasive Blood Pressure (PCG)

Time	PCG Mentah	PCG Kalman	PCG Butterworth
14.18,8	1,23	2,43	3,64
14.18,9	1,17	2,39	3,62
14.18,9	1,3	2,46	3,55
14.18,9	1,18	2,41	3,73
14.18,9	1,33	2,48	3,58
14.18,9	1,08	2,36	3,75
14.18,9	1,43	2,53	3,44
14.18,9	1,03	2,34	3,9
14.18,9	1,33	2,46	3,34
14.19,0	1,15	2,39	3,77
14.19,0	1,24	2,42	3,52
14.19,0	1,22	2,42	3,65
14.19,0	1,25	2,44	3,62
...	...	...	...
Mean	1,22698	2,4265	3,62454

At each listed time point, there is a variation in the amplitude of the signal produced by each processing method. The raw PCG signal, which has not undergone any filtering, has the lowest amplitude values, with an average of about 1.22698. After applying the Kalman filter, the average amplitude increases to approximately 2.4265, indicating that this filter has reduced noise in the signal and smoothed the amplitude fluctuations. The application of the Butterworth filter further increases the average amplitude to around 3.62454, suggesting that this filter processes the signal differently, possibly with more aggressive noise reduction or enhancement of certain signal components.

### C. Correlation between ECG, PCG, and NIBP through Data Collection on 10 Respondents

To explore the relationship between these three parameters, a comprehensive testing procedure was conducted involving 10 respondents. This study will focus on a detailed analysis of the R peak in the electrocardiogram (ECG) alongside the first and second heart sounds (S1 and S2), as well as the systolic and diastolic intervals measured through phonocardiogram (PCG). By examining these specific elements, we aim to uncover potential correlations that may enhance our understanding of cardiovascular dynamics and their implications in clinical settings.

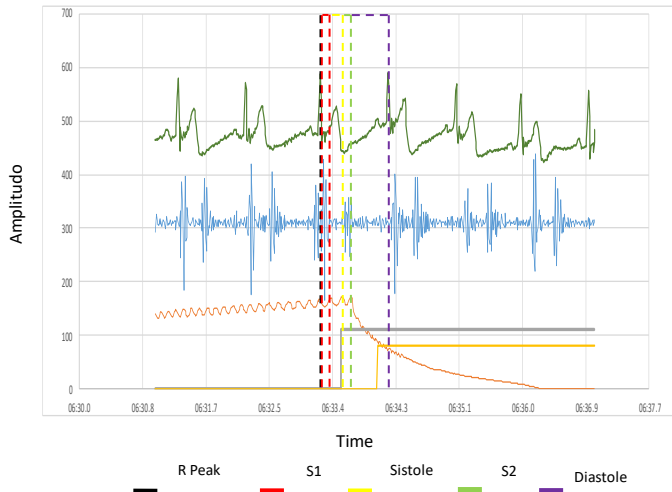


Fig. 8. Correlation Signal between ECG, PCG with NIBP (Systole and Diastole) in research exploration of Digital Filter on Cardiac Monitor Equipped with Non-Invasive Blood Pressure in Data Streamer Excel

Figure 8 is a signal display of 3 parameters: electrocardiograph (green), phonocardiograph (blue), and blood pressure (orange). It showed a significant correlation between the R peak in the ECG signal, the first (S1) and second (S2) heart sounds in the PCG signal, and systolic and diastolic blood pressure measured using a non-invasive blood pressure monitor (NIBP). The gray straight line indicates the reading of systole pressure and the light orange straight line indicates the reading of diastole pressure. The dashed lines are the distance and time identification boundaries to determine peak R (black), S1 (red), S2 (yellow), systole interval (green), and diastole interval (purple). After the first heart sound, the signal starts to get smaller, indicating a pause towards the second heart sound called the systole interval. When the signal starts to grow larger again, it indicates the second heart sound, and then the signal shrinks again with a slightly longer period of time than the systole interval. This is called the diastole interval, which is the interval from the second heart sound to the first heart sound. The information obtained from the visualization process of normal heart sounds are.

Table 4. Overall Correlation Results of 10 Respondents in Respondents in Research Exploration of Digital Filter on Cardiac Monitor Equipped with Non-Invasive Blood Pressure

Resp	R Peak (ECG)	S1 (PCG)	S2 (PCG)	Interval Systol	Interval Diastol
1	0,02	0,11	0,10	0,15	0,51
2	0,08	0,20	0,14	0,12	0,50
3	0,01	0,10	0,12	0,14	0,48
4	0,01	0,15	0,10	0,16	0,47
5	0,01	0,12	0,11	0,14	0,52

6	0,02	0,10	0,09	0,11	0,31
7	0,02	0,10	0,08	0,11	0,37
8	0,04	0,09	0,07	0,09	0,33
9	0,03	0,10	0,07	0,15	0,32
10	0,02	0,09	0,07	0,13	0,27
Average	0,02	0,11	0,09	0,13	0,40

Table 4 displays the results of the duration of the first heart sound, second heart sound, systole interval, diastole interval, and the appearance of the R peak of the ECG obtained from 10 respondents. The duration of the first heart sound was 0.09-0.2s. The duration of the second heart sound was faster than the first heart sound, which was 0.07-0.14s. The systole interval was 0.09-0.16s. The appearance of the diastole interval is 0.27-0.52s. And finally, the time interval of the appearance of peak R with the first heart sound is 0.09-0.2s.

#### D. Comparison of Blood Pressure Measurement Results Using The Device with The Algorithm Estimation Formula

This comparison was performed to determine how accurate the designed device was in measuring blood pressure, by comparing results using algorithmic estimation formulas found in previous studies. The choice of this formula was motivated by the relatively low error rate compared to some other studies.

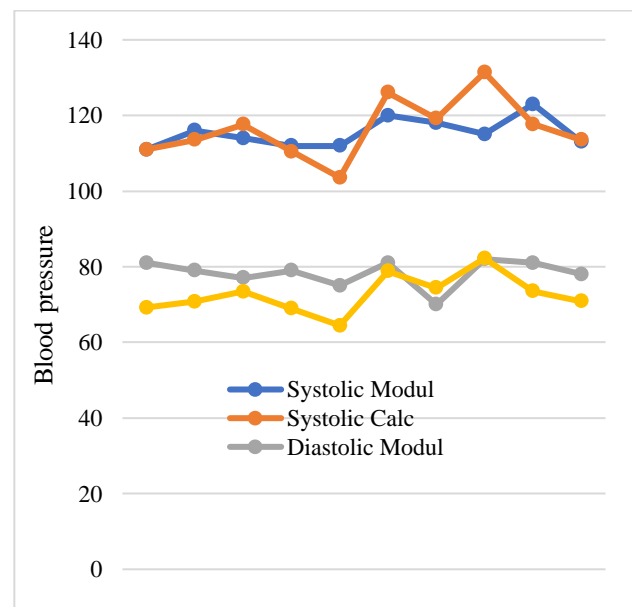


Fig. 9. Comparison of systolic and diastolic blood pressure measurements between Modul and Calc values across ten measurement instances.

Figure 9 is a comparison graph of systolic and diastolic measurements between the module and the device. The

graph shows that the measurement values obtained by the device are not significantly different from those measured by the module, indicating that the device demonstrates a fair level of accuracy.

**Table 5.** Comparison Table of Blood Pressure Measurement Results using the Module with Estimated Calculations

Resp	Systolic (Mean)			Diastolic (Mean)		
	Modul	Calc	Error	Modul	Calc	Error
1	111	110,98	0,02	81	69,2	11,8
2	116	113,53	2,47	79	70,82	8,18
3	114	117,56	3,56	77	73,4	3,6
4	112	110,5	1,5	79	68,89	10,11
5	112	103,57	8,43	75	64,47	10,53
6	120	126,05	6,05	81	78,82	2,18
7	118	119,2	1,2	70	74,44	4,44
8	115	131,37	16,37	82	82,21	0,21
9	123	117,7	5,3	81	73,49	7,51
10	113	113,56	0,56	78	70,84	7,16
Mean Total		4,546			6,572	
Std		4,942464972			3,836511147	

**Table 5** compares blood pressure measurement results using the module device with the algorithm estimation formula on 10 respondents for 5 times of data collection. This table shows the results obtained, the largest difference in systole is 16.37 mmHg. Meanwhile, the largest difference in diastole is 11.8 mmHg. With a mean at systole of 4.546 and a standard deviation of 4.942464972. In diastole, the mean is 6.572 and the standard deviation is 3.836511. This shows that the developed device is quite accurate in measuring blood pressure, although there were some anomalies in some subjects that need further exploration.

The results of this study indicate that the 8th order Butterworth filter is the best choice in reducing noise in ECG and PCG signals, especially at high frequencies. However, its use must be carefully considered so as not to eliminate important information at low frequencies. Although the Kalman filter has been shown to be effective at some frequencies, its effectiveness is not comparable to Butterworth in the context of this study.

#### 4. DISCUSSION

After testing the heart monitor module, data was collected and analyzed to assess the accuracy and performance of the module in monitoring heart development. This study also aims to evaluate the impact of digital filters in reducing noise. The digital filters used are the Kalman

filter and Butterworth filters (order 2, 4, and 8). The results of the analysis from the research and testing of the Heart Monitor device include the heart signals before and after the addition of digital filters, displayed through FFT to show the amplitude and frequency of ECG and PCG signals.

In the ECG results, at low frequencies (0.5 Hz and 5 Hz), Butterworth filters of orders 2, 4, and 8 show varying reductions in amplitude. At 0.5 Hz, the amplitude of the signal after filtration with filter order 2 is 350.06, while orders 4 and 8 produce amplitudes of 330.9 and 238.8, respectively, indicating noise suppression. However, the difference between filters of orders 4 and 8 is relatively small, suggesting that increasing the filter order does not significantly affect noise reduction at low frequencies. At 5 Hz, the amplitude of the signal after filtration is 474 for order 2, with a relatively minor reduction in filters of orders 4 and 8, which produce amplitudes of 453.72 and 449.87. At intermediate frequencies (30 Hz and 40 Hz), filters with higher orders start to show superiority in noise reduction. At 30 Hz, filter order 2 reduces the amplitude to 445.89, while filters of orders 4 and 8 reduce the amplitude to 425.65 and 412, respectively. This trend continues at 40 Hz, where filter order 2 produces an amplitude of 412.56, while orders 4 and 8 produce amplitudes of 393.87 and 387.69, indicating the effectiveness of higher-order filters in reducing noise at intermediate frequencies.

At high frequencies (80 Hz to 120 Hz), filter order 8 consistently demonstrates superior capability in reducing signal amplitude. For example, at 80 Hz, filter order 2 produces an amplitude of 320.49, filter order 4 produces 298.65, and filter order 8 produces 198.82. At 120 Hz, the amplitude of the signal after filtration with filter order 8 decreases drastically to 18.89, compared to 64.98 for order 4 and 108.65 for order 2. These results show that Butterworth filter order 8 is highly effective in suppressing high-frequency noise in ECG signals, supported by the PSD results in Figure 4. Butterworth filter order 8 provides the lowest PSD result (-56.978 dB), indicating the best effectiveness in noise suppression among the three filters tested. A lower PSD value signifies that filter order 8 is more effective in reducing noise strength and, thus better in cleaning the signal from unwanted components.

Implementation of the Kalman filter on low-frequency ECG signals (0.5 Hz and 5 Hz) shows that all Kalman filter configurations (R:10; Q:1, R:1; Q:1, and R:1; Q:0.1) produce similar results, closely matching the original amplitude with minimal noise reduction. At mid-range frequencies (30 Hz), the R:1; Q:1 configuration demonstrates better performance with an amplitude of 482.65 compared to R:10; Q:1 (435.91) and R:1; Q:0.1

(430), indicating more effective noise suppression. For high frequencies (60 Hz to 100 Hz), the R:1; Q:1 configuration continues to perform well, producing amplitudes closer to the original signal compared to R:10; Q:1 and R:1; Q:0.1. For example, at 100 Hz, R:1; Q:1 yields 421.76, while R:10; Q:1 and R:1; Q:0.1 yield 247.2 and 221.24, respectively. This indicates that R:1; Q:0.1 provide a good balance between noise reduction and signal preservation, especially at higher frequencies. The PSD results shown in FIGURE 6 demonstrate that the Kalman filter configuration with R:1; Q:0.1 yields the lowest PSD (-31.73 dB), indicating the best noise suppression among the three configurations. A more negative PSD value indicates that this filter is the most effective in reducing noise power.

Results for PCG signals show that the PCG signal only has frequencies below 30 Hz, with varying baseline drops at each filter order. Through amplitude analysis, it was found that adding Butterworth filter order 8 to the PCG signal minimizes noise and increases amplitude, allowing the PCG signal to be digitized with a higher amplitude. The average amplitude after adding Butterworth filter order 8 is 3.62454, compared to the average amplitude using the Kalman filter of 2.4265, making the PCG signal clearer and easier to analyze.

The results obtained after experimenting with the addition of digital filters on heartbeat signals and heart sound signals are as follows. Butterworth order 8 is the best digital filter for reducing noise in this study on heart rate signals and heart sound signals[28][29]. Adding a Butterworth filter to these two heart signals produces a smoother signal than the signal that has not been given a digital filter. Meanwhile, the addition of the Kalman filter to the heartbeat signal and heart sound signal resulted in some signals disappearing, causing the signal to be abnormal. Kalman filter is a state estimation technique[30][31], the application of Kalman filter in this study is to reduce the noise detected through the AD8232 sensor and GYMAX9814 sensor. The comparison simulation results show that the 8th-order Butterworth is better at reducing noise than the Kalman filter. The inefficient performance of the Kalman filter is due to its limited applicability[32]. Depending on the desired application purpose, the Kalman filter can work well[33][34].

NIBP results are shown in TABLE 4, which includes the response time of the first heart sound, the second heart sound, systolic interval, diastolic interval, and heart rate based on the appearance of the R peak. The time interval between the start and end of the signal is the time duration used as a reference to state the suitability of the

relationship between the three parameters when displayed simultaneously. From these results, it was found that the duration of the first heart sound signal was 0.15s. The duration of the second heart sound signal is 0.12s. The duration of the systole interval is 0.15s. The duration of the diastole interval was 0.51s and the time when the R peak appeared on the ECG was 33.28 seconds. Based on the data obtained, the duration of S1, S2 and the diastole interval are still within the duration limits, namely the duration of S1 is 70-150ms, the duration of S2 is 60-120ms, the duration of the diastole interval is 500ms[35]. So it can be stated that this research and the research conducted by Nelika[35] have the same and appropriate statements. Meanwhile, the duration of S1, S2, systole interval, and diastole interval are also still within the duration limits stated by Chengyu Liu[36]. The appearance time of S1 is 10ms after the appearance of QRS, this has the same statement as Xin Qi Bao[37]. FIGURE 8 shows the appearance of the second heart sound (S2) which occurs towards the end of the T wave in the heartbeat signal (ECG). This research has similarities with research conducted by Suranan Noimanee [38]. And the duration of S2 obtained from this research is also similar to research conducted by AF Quiceno[39]. The green and orange lines are automatic readings of blood pressure via motorized pumping. The green line shows the systolic pressure. Meanwhile, the orange color shows diastolic pressure. Through this line shows evidence of a strong correlation between blood pressure with heart rate and heart sounds[4]. Systolic and diastolic pressures are read precisely in the systolic interval and diastolic interval, where the systolic interval is between the first and second heart sounds while the diastolic interval is between the second and first heart sounds[40]. In addition, the systolic and diastolic pressures are read exactly between the RST complex on the ECG for systolic pressure and the diastolic pressure between the U wave and the R peak on the ECG, which is in accordance with Christer Ahlstrom's research[41]. In the previous table 3, the error value obtained was shown. The large difference between the module and calculation results is due to the fact that the estimation algorithm used as reference for the calculation has an error rate in the estimation of systolic and diastolic blood pressure of  $6.48 \pm 4.48$  mmHg and  $3.91 \pm 2.58$  mmHg. Meanwhile, in this study, the obtained systolic and diastolic blood pressure errors were  $4.54 \pm 4.94$  mmHg and  $6.57 \pm 3.83$  mmHg. The error rate remained within the AAMI standard limit of  $5 \pm 8$  mmHg[42].

Due to various factors, the module made by researchers is far from perfect, both in terms of planning, manufacturing, and how the module works. Therefore, the researchers analyzed several shortcomings in this

research as follows. The first is that the results of this study can only display results through a PC that has been connected using a USB cable so that without using a connecting cable, the module cannot work. Second, there is a delay that affects the reading of ECG and BPM signals. Third, the PCG signal still shows noise, this is due to the sensitive sensor that requires additional circuits so as not to cause noise in the surrounding environment to be heard. Fourth, the pressure sensor affects the data reading results when compared to the calibrated device. The signal detected in the previous study was the original signal without a digital filter, so there was a possibility of noise due to the sensitive nature of the module and not equipped with a blood pressure gauge. Whereas in this study, a digital filter is added to the ECG and PCG signals and equipped with a blood pressure measurement so that monitoring of the patient's heart condition is better and more precise in diagnosing, and early prevention can be done[4].

Several previous studies[19][41][43] have discussed the correlation between ECG, PCG, and NIBP, these studies have the same conclusion where there is a correlation between these three parameters. However, each study has different time durations for the first heart sound (S1), second heart sound (S2), systolic interval, diastolic interval, and time of appearance of the R peak on the ECG. This is because each heartbeat, heart sound and blood pressure in each subject is different, resulting in different time durations[38][44]. Research[4][12][13][14] has conducted research on each parameter, which has the same results as the current study. However, it does not account for ECG, PCG, and NIBP parameters simultaneously and does not provide digital filters to improve signal and module performance. Based on the problems and studies that have been carried out, the researchers conducted research entitled "Exploration of Digital Filters on Cardiac Monitor Devices Equipped with NIBP" which aims to develop a device to monitor heart parameters, heart monitor parameters for ECG, PCG, and NIBP by displaying the signals simultaneously. In this study, further observations were also made to determine the relationship between ECG, PCG, and NIBP.

In addition, this research advances and improves upon previous studies [14] by incorporating blood pressure readings. Additionally, this study introduces digital filters to heart sound signals and features a more minimalist design that enhances the comfort of operating the device compared to earlier research [4]. The benefits of this research include the development of a tool for monitoring heart conditions through recording heart rate (ECG) and heart sounds (PCG), which has been enhanced by adding digital filters and blood pressure measurements. By analyzing the addition of digital filters to PCG and ECG signals, this study aims to provide deeper insights and knowledge into the exploration of digital filters in cardiac monitors to determine the best

digital filters applicable to the signals. Furthermore, it is expected to enrich understanding of the relationship between heart rate, heart sounds, and blood pressure. In this study, the use of digital filters on cardiac signals, especially ECG and PCG, provided significant results in reducing interference and improving signal quality. However, there are several limitations that need to be considered to strengthen the analysis results. First, the sample size of the study, which only consisted of 10 respondents aged 18-24 years, is one of the main limitations. This small sample size and lack of demographic variation can affect the external validity of the study, so that the results obtained may not be generalizable to a wider population or different age groups.

In addition, confounding factors such as environmental degradation and technical measurements in sensor devices need more attention. Although Butterworth and Kalman filters successfully reduced signal degradation, environmental conditions and sensor sensitivity can affect measurement accuracy. Further analysis of how the device can perform under varying environmental conditions will enrich the results and provide a more comprehensive understanding of the performance of this device in the real world.

In addition, although the 8th-order Butterworth filter is more effective in reducing high-frequency noise compared to the Kalman filter, improvements in hardware and software design are still needed to minimize other confounding factors such as pressure variations and mechanical disturbances from the environment. This will help ensure that the developed device can produce clean and accurate signals for a variety of patient conditions.

In the future, research can be developed by expanding the sample size and conducting trials in more diverse age groups. Research also needs to further explore the use of this technology in real clinical contexts to ensure wider application. In conclusion, although this device shows great potential in non-invasive cardiac monitoring, further research is needed to measure its performance outside the laboratory.

## 5. CONCLUSION

The purpose of this research is to develop a device to monitor cardiac parameters, cardiac monitor parameters for ECG, PCG, and NIBP by displaying signals simultaneously and further observations are also made to determine the relationship between ECG, PCG, and NIBP. Based on the research conducted, the following conclusions can be drawn:

1. A cardiac monitor device has been successfully developed using the AD8232, GYMAX9814, and MPX5050GP modules, capable of monitoring ECG and PCG parameters and measuring NIBP blood pressure.

- The 8th-order Butterworth filter has proven to be the most effective at reducing noise at high frequencies compared to the Kalman filter. While the Kalman filter is effective at medium frequencies, the 8th-order Butterworth filter delivers superior results for ECG and PCG signals, enhancing signal quality and blood pressure measurement accuracy.
- Blood pressure measurement can be conducted through ECG and PCG signal recording, with systolic and diastolic blood pressure estimation errors of  $4.54 \pm 4.94$  mmHg and  $6.57 \pm 3.83$  mmHg, respectively, which are within the AAMI standard limits of  $5 \pm 8$  mmHg.

The results obtained state that the device has worked well and can work according to its work function and the standards set. The potential impact on clinical practice of the development of this tool is significant. This research has the advantage of a more minimalist tool design. In addition, this research applies digital filters to ECG and PCG signals, resulting in better signals. This research has been developed, which is equipped with NIBP blood pressure measurement as the main measurement in diagnosing the patient's initial condition.

This study has successfully developed a cardiac monitoring device with digital filter integration that can improve the quality of ECG and PCG signals, as well as non-invasive blood pressure (NIBP) measurements. The results showed that the 8th-order Butterworth filter was significantly more effective in reducing noise at high frequencies, while the Kalman filter also showed effectiveness at mid-frequency. The resulting blood pressure measurements were in accordance with the AAMI standard, with an acceptable error rate.

However, this conclusion does not fully cover the potential clinical applications of the developed device. This technology has great potential for use in real-time cardiac monitoring in clinical settings, especially in the early detection and management of heart disease. To ensure wider application, future research should focus on trials with larger and more diverse populations, as well as testing in various clinical conditions.

To overcome the limitations of the current study, steps are needed such as expanding the sample size to include more diverse age groups and conducting tests in more varied environmental conditions. In addition, improvements in hardware design, including the use of sensors that are more resistant to environmental interference, can improve measurement accuracy. Device development also needs to integrate wireless communication technologies to enable remote monitoring without the reliance on wired connections, facilitating implementation in both clinical and home settings.

Further development could also include integrating the device with telemedicine technologies for remote patient monitoring, which has significant implications for patient care and reducing the burden on healthcare systems.

## REFERENCES

- M. Mitra, "Cardiac Monitoring to aid in Diagnosis," no. December, 2020, doi: 10.35877/454RI.jinav156.
- R. Jessica K. Zègre-Hemsey, PhD, RN, J. Lee Garvey, MD, and Mary G. Carey, PhD, "Cardiac Monitoring in the Emergency Department Jessica," *HHS Public Access*, vol. 28, no. 3, pp. 331–345, 2017, doi: 10.1016/j.cnc.2016.04.009.Cardiac.
- Medtronic, "Heart Monitoring," 2018. <https://www.medtronic.com/us-en/patients/treatments-therapies/insertable-heart-monitors/getting-monitor.html>
- R. Alvionita *et al.*, "Design of Cardiac Monitor for Multi Parameters," *Proc. - 2019 Int. Semin. Appl. Technol. Inf. Commun. Ind. 4.0 Retrospect. Prospect. Challenges, iSemantic 2019*, pp. 423–428, 2019, doi: 10.1109/ISEMANTIC.2019.8884264.
- Amit Sapra; Ahmad Malik; Priyanka Bhandari, *Vital Sign Assessment*. StatPearls, 2023. [Online]. Available: <https://www.ncbi.nlm.nih.gov/books/NBK553213/>
- T. P. Craig Lockwood, Tiffany Conroy -Hiller, "Vital Signs," *Natl. Libr. Med.*, vol. 2, no. 6, pp. 1–38, 2004, doi: 10.1112/01938924-200402060-00001.
- J. E. Stevenson, J. Israelsson, G. Petersson, and P. A. Bath, "Factors influencing the quality of vital sign data in electronic health records: A qualitative study," *J. Clin. Nurs.*, vol. 27, no. 5–6, pp. 1276–1286, 2018, doi: 10.1111/jocn.14174.
- U. Suriepto and J. Utama, "Telemonitoring Elektrokardiografi Portabel Portable Electrocardiograph Telemonitoring," *Semant. Sch.*, vol. 2, no. 1, 2014, [Online]. Available: <https://www.semanticscholar.org/paper/Telemonitoring-Elektrokardiografi-Portabel-Portable-Utama/91b910fd9fae09e61cca35aca2bc2d8ecb5e0e4>
- Anand Kumar Joshi; Arun Tomar; Mangesh Tomar, "A Review Paper on Analysis of Electrocardiograph (ECG) Signal for the Detection of Arrhythmia Abnormalities," *ResearchGate*, vol. 3, no. 10, pp. 12466–12475, 2014, doi: 10.15662/ijareeie.2014.0310028.
- A. Pal, A. K. Gautam, and Y. N. Singh, "Evaluation of bioelectric signals for human recognition," *Procedia Comput. Sci.*, vol. 48, no. C, pp. 746–752, 2015, doi: 10.1016/j.procs.2015.04.211.
- C. Saxena, A. Sharma, R. Srivastav, and H. K. Gupta, "Denosing of ECG signals using FIR & IIR filter: A performance analysis," *Int. J. Eng. Technol.*, vol. 7, no. 4.12 Special Issue 12, pp. 1–5, 2018, doi: 10.14419/ijet.v7i4.12.20982.
- U. Machine and L. Techniques, "Non-Invasive Blood Pressure Estimation from ECG Using Machine Learning Techniques," pp. 1–20, 2018, doi: 10.3390/s18041160.
- T. Le *et al.*, "Continuous Non-Invasive Blood Pressure Monitoring: A Methodological Review on Measurement Techniques," *IEEE Access*, vol. 8, pp. 212478–212498, 2020, doi: 10.1109/ACCESS.2020.3040257.
- A. R. Masnulula and H. G. Ariswati, "Development of Cardiac Monitor Using Piezoelectric Through Carotid Pulse," vol. 1, no. 1, 2021.
- Smart Health, "Phonocardiography," 2022. [https://www.sciencedirect.com/topics/medicine-and-dentistry/phonocardiography#:~:text=A+phonocardiogram+\(PCG\)+plots+recordings,%2C+%26+Nanayakkara%2C+2021](https://www.sciencedirect.com/topics/medicine-and-dentistry/phonocardiography#:~:text=A+phonocardiogram+(PCG)+plots+recordings,%2C+%26+Nanayakkara%2C+2021). (accessed Sep. 30, 2023).
- Sean Dornbush; Andre E. Turnquest, "Physiology, Heart Sounds," *StatPearls*, 2023.
- R. C. Peng, W. R. Yan, N. L. Zhang, W. H. Lin, X. L. Zhou, and Y. T. Zhang, "Cuffless and Continuous Blood Pressure Estimation from the Heart Sound Signals," *Sensors*, vol. 15, no. 9, pp. 23653–23666, 2015, doi: 10.3390/S150923653.
- J. Li, L. Ke, Q. Du, X. Ding, and X. Chen, "Research on the Classification of ECG and PCG Signals Based on BiLSTM-

**Corresponding author:** Elmira Rofida Alhaq, [elmirarofida.a@gmail.com](mailto:elmirarofida.a@gmail.com), Department of Medical Electronics Technology, Poltekkes Kemenkes Surabaya, Jl. Pucang Jajar Timur No. 10, 60282, Surabaya, Indonesia and Biomedical Engineering Master Degree, Departement of Physics, Faculty of Science and Technology, Surabaya, Indonesia.

**Copyright** © 2024 by the authors. Published by Jurusan Teknik Elektromedik, Politeknik Kesehatan Kemenkes Surabaya Indonesia. This work is an open-access article and licensed under a Creative Commons Attribution-ShareAlike 4.0 International License ([CC BY-SA 4.0](https://creativecommons.org/licenses/by-sa/4.0/)).

- GoogLeNet-DS," *Appl. Sci.*, vol. 12, no. 22, 2022, doi: 10.3390/app122211762.
- [19] A. K. Abbas and R. Bassam, "Phonocardiography Signal Processing," *Synth. Lect. Biomed. Eng.*, vol. 31, no. May, pp. 1–189, 2009, doi: 10.2200/S00187ED1V01Y200904BME031.
- [20] A. Esmaili, M. Kachuee, and M. Shabany, "Non-invasive Blood Pressure Estimation Using Phonocardiogram," pp. 5–8, 2017, doi: 10.1109/ISCAS.2017.8050240.
- [21] M. Shouran and E. Elgamli, "Design and Implementation of Butterworth Filter," *Int. J. Innov. Res. Sci. Eng. Technol.*, 2020, [Online]. Available: [www.ijirset.com](http://www.ijirset.com)
- [22] J. Wang, X. Geng, and J. Xu, "Nonlinear Kalman Filtering based on Self-Attention Mechanism and Lattice Trajectory Piecewise Linear Approximation," 2024, [Online]. Available: <http://arxiv.org/abs/2404.03915>
- [23] U. Pratiwi, I. Fadli, W. T. Cahyanto, and Hartono, "Implementation of Kalman Filter Algorithm To Optimize the Calculation of Ultrasonic Sensor Distance Value in Hooke Law Props System," *Eastern-European J. Enterp. Technol.*, vol. 1, no. 5(127), pp. 48–60, 2024, doi: 10.15587/1729-4061.2024.296667.
- [24] M. B. S. Sugunakar, K. N. Maruthy, C. H. Srinivas, and P. Johnson, "A comparative study between single lead AD8232 heart rate monitor and standard electrocardiogram to acquire electrocardiographic data for cardiac autonomic function testing," *Indian J. Sci. Technol.*, vol. 14, no. 6, pp. 534–540, 2021, doi: 10.17485/ijst/v14i6.1822.
- [25] Maxim Integrated, "Microphone Amplifier with AGC and Low-Noise MAX9814," *Analog Device*, pp. 1–14, 2009, [Online]. Available: <https://datasheets.maximintegrated.com/en/ds/MAX9814.pdf>
- [26] S. O. Ardila, E. Yulianto, and S. Sumber, "Digital ECG Phantom Design to Represent the Human Heart Signal for Early Test on ECG Machine in Hospital," *Int. J. Adv. Heal. Sci. Technol.*, vol. 1, no. 1, pp. 14–19, 2021, doi: 10.35882/ijahst.v1i1.3.
- [27] Rigel Medical, "Rigel UNI-SIM: Hand-Held Vital Signs Simulator - Instruction Manual," vol. 44, no. 1, pp. 0–1, 2010.
- [28] I. D. Gede, H. Wisana, P. C. Nugraha, and R. A. Rachman, "Development of a Low-Cost and Efficient ECG devices with IIR Digital Filter Design," vol. 3, no. 1, pp. 21–28, 2021.
- [29] N. R. Saputri and S. Luthfiyah, "Enhancing the Electrocardiogram Signal Quality by Applying Butterworth Infinite Impulse Response Filter 8 th Order," 2022.
- [30] Q. Li, R. Li, K. Ji, and W. Dai, "Kalman Filter and Its Application," no. 10, pp. 74–77, 2015, doi: 10.1109/ICINIS.2015.35.
- [31] D. S. Fussell, "An Elementary Introduction to Kalman Filtering," pp. 6–11, 1960.
- [32] B. R. Manju, "ECG Denoising Using Wiener Filter and Kalman Filter ECG Denoising Using Wiener Filter and Kalman Filter," *Procedia Comput. Sci.*, vol. 171, no. 2019, pp. 273–281, 2020, doi: 10.1016/j.procs.2020.04.029.
- [33] V. R. R. D, A. R. B, and F. Shaik, "Gaussian Noise Filtering From ECG Signal Using Improved Kalman Filter," vol. 3, no. 2, pp. 118–126, 2015.
- [34] Shussain Salleh; Tian Swee Tan; Siti Hadrina Sh Hussain; Chee Ming Ting, "Acoustic cardiac signals analysis : a Kalman filter – based approach," *ResearchGate*, no. May 2014, 2012, doi: 10.2147/IJN.S32315.
- [35] V. N. Varghees and K. I. Ramachandran, "A novel heart sound activity detection framework for automated heart sound analysis Biomedical Signal Processing and Control Short Communication A novel heart sound activity detection framework for automated heart sound analysis," *Biomed. Signal Process. Control*, vol. 13, no. September, pp. 174–188, 2014, doi: 10.1016/j.bspc.2014.05.002.
- [36] C. Liu, D. Springer, Q. Li, B. Moody, R. A. Juan, and F. J. Chorro, "An Open Access Database for the Evaluation of Heart Sound Algorithms," no. November, 2016, doi: 10.1088/0967-3334/37/12/2181.
- [37] X. Bao, Y. Deng, and E. N. Kamavuako, "Analysis of ECG and PCG Time Delay around Auscultation Sites Analysis of ECG and PCG Time Delay around Auscultation Sites," no. January, 2020, doi: 10.5220/0008942602060213.
- [38] S. Noimanee, T. Tunkasiri, K. Siriwitayakorn, and J. Tantrakoon, "Piezoelectric Ceramics Sensor Based on the Computerization," pp. 3192–3208, 2007.
- [39] A. F. Quiceno, E. Delgado, M. Vallverd, A. M. Matijasevic, and G. Castellanos-Domnguez, "Effective phonocardiogram segmentation using nonlinear dynamic analysis and high-frequency decomposition," *Comput. Cardiol.*, vol. 35, pp. 161–164, 2008, doi: 10.1109/CIC.2008.4749002.
- [40] M. F. Syahputra, R. F. Rahmat, and J. A. Sitepu, "Visualisasi Suara Jantung Manusia Pada Platform Mobile," *Lentera*, vol. 15, no. 6, pp. 66–72, 2015.
- [41] C. Ahlström, *Nonlinear Phonocardiographic Signal Processing*, no. 1168. 2008. [Online]. Available: <http://sh.diva-portal.org/smash/record.jsf?pid=diva2:17719>
- [42] "Association for the Advancement of Medical Instrumentation et al. American national standard. manual, electronic or automated sphygmomanometers.," vol. ANSI/AAMI.
- [43] B. Soroor, "A hybrid algorithm for heart sounds segmentation based on phonocardiogram Soroor Behbahani," *J. Med. Eng. Technol.*, vol. 43, no. 6, pp. 363–377, 2019, doi: 10.1080/03091902.2019.1676321.
- [44] "Heart Sounds Topic Review," *Heal. Learn Hear.*, [Online]. Available: <https://www.healio.com/cardiology/learn-the-heart/cardiology-review/topic-reviews/heart-sounds>